IJST (2014) 38A3: 265-279
Iranian Journal of Science & Technology

http://ijsts.shirazu.ac.ir

Dynamics and bifurcations of a Lotka-Volterra population model

R. Khoshsiar Ghaziani

Department of Applied Mathematics, Shahrekord University, P. O. Box 115, Shahrekord, Iran
E-mail: Khoshsiar@sci.sku.ac.ir

Abstract

This paper investigates the dynamics and stability properties of a discrete-time Lotka-Volterra type system. We first analyze stability of the fixed points and the existence of local bifurcations. Our analysis shows the presence of rich variety of local bifurcations, namely, stable fixed points; in which population numbers remain constant, periodic cycles; in which population numbers oscillate among a finite number of values; quasi-periodic cycles; which are constraint to stable attractor called invariant closed curve, and chaos, where population numbers change erratically. Our study is based on the numerical continuation method under variation of one and two parameters and computing different bifurcation curves of the system and its iterations. For the all codimension 1 and codimension 2 bifurcation points, we compute the corresponding normal form coefficients to reveal criticality of the corresponding bifurcations as well as to identify different bifurcation curves which emerge around the corresponding bifurcation point. In particular we compute a dense array of resonance Arnol'd tongue corresponding to quasi-periodic invariant circles rooted in weakly resonant Neimark-Sacker associated to multiplier $\lambda = e^{2\pi qi}$ with frequency $q = \frac{2}{5}$. We further perform numerical simulations to characterize qualitatively different dynamical behaviors within each regime of parameter space.

Keywords: Normal forms; stable cycles; codimension of bifurcation; center manifold

1. Introduction

It is well known that the Lotka-Volterra prey-predator model is one of the fundamental population models. This model is described by the following system of ordinary differential equations:

$$\begin{aligned} \dot{x}(t) &= xq(x) - \alpha yp(x), \\ \dot{y}(t) &= (p(x) - \beta)y, \end{aligned} \tag{1}$$

where x, y represent the prey and predator density, respectively. $p(x)$ is the predator functional response and α, $\beta > 0$ are the conversion and predator's death rates, respectively.

Since the pioneering theoretical works by Lotka (1956) and Volterra (1962) in the last century, the study of more realistic prey-predator models was introduced by Holling, suggesting three kinds of functional responses for different species for modeling the phenomena of predation (Holling, 1965). The research dealing with specific interactions has mainly focused on continuous prey-predator models of two variables, where the dynamics include only stable equilibrium or limit cycles (Freedman and Mathsen, 1993; Hasting, 1981; Kooij and Zegeling, 1997; Lindstrom, 1993; Rosenzweig and MacArthur, 1963). Since then, the dynamic relation between predator and prey has become one of the dominant themes in both ecology and mathematical ecology due to its universal existence and importance (Jiao et al., 2008a; Jiao et al., 2008b; Wang et al., 2007; Zeng et al., 2008). However, in recent years many authors (Agarwal, 2000; Cai and Huang, 2013; Dawes and Souza, 2013; Freedman, 1980; Goh, 1980; He and Lai, 2011; Jing and Yang, 2006; Kuang, 1993; Liu and Xiao, 2007; Murray, 1993; Wang et al., 2013) have suggested that discrete-time models are more appropriate than the continuous ones, especially when the populations have non-overlapping generations. Furthermore, discrete- time models often provide very effective approximations to continuous models which cannot be solved explicitly. Periodic forcing, may also affect predator and prey. It is known that dynamical systems with simple dynamical behavior in the constant parameter case display very complex behavior including chaos when they are periodically perturbed (Agiza et al., 2009; Beddington et al., 1975; Blackmore et al., 2001; Danca et al., 1997; Hastings, 1981).

In this paper, we consider the Lotka-Volterra type predator-prey system which was introduced in

Received: 16 July 2013 / Accepted: 16 April 2014

(Brauer and Castillo-Chavez, 2001) and (Rosenzweig and MacArthur, 1963)

$$\begin{aligned}\dot{x}(t) &= rx(1 - x) - bxy,\\ \dot{y}(t) &= (-d + bx)y,\end{aligned} \tag{2}$$

where r, b and d are positive parameters.
Applying the forward Euler scheme to system (1) we obtain the discrete system

$$F:\begin{pmatrix}x\\ y\end{pmatrix}\mapsto\begin{pmatrix}x+\delta(rx(1-x)-bxy)\\ y+\delta(-d+bx)y\end{pmatrix}, \tag{3}$$

where δ is the step size.

We will generally choose b, δ as the unfolding parameters in the bifurcation study. To some extent, it is the simplest possible discrete predator-prey model, and therefore allows a reasonably complete analytical treatment as far as the fixed points of the map are concerned. However, we will see that even in this case the behavior of cycles is very complicated and can only be studied by numerical methods.

This paper is organized as follows. In Section 2, we recall some results on the bifurcation analysis of periodic orbits of discrete maps. In particular, we give some results on normal forms of codim-1 and codim-2 bifurcations of fixed point of maps. In Section 3, we discuss the stability and bifurcation of the fixed points of the map (3). We derive analytically the stability regions of fixed points and their bifurcation behaviors. Moreover, we compute analytically the critical normal form coefficients in the case of the period doubling bifurcation to prove super criticality. Next, in Section 4, we numerically compute curves of fixed points and bifurcation curves of the map and its iterates under variation of one and two parameters. We compute the critical normal form coefficients of all computed codim-1 and codim-2 bifurcations. These coefficients are powerful tools to compute stability boundaries of the map and its iterates. In particular, we determine the bifurcation scenario of the map near an R4 resonance point, which involves stable and unstable 4-cycles as well as 8-cycles and 16-cycles. We further compute an Arnold's tongue of period 5 and so find a parameter region where stable period-5 cycles exist. In this section, we also do numerical simulations to reveal more complex behavior of the system near a resonance R4 point. We conclude our work in Section 5 with a discussion of the obtained results.

2. Some aspects of the bifurcation of cycles of maps

We consider a smooth map

$$x \mapsto f(x,\alpha), \tag{4}$$

where $x \in \mathbb{R}^n$ is a state variable vector and $\alpha \in \mathbb{R}^p$ is a parameter vector. Write the K-th iterate of (4) at some parameter value as

$$x \mapsto f^{(K)}(x,\alpha),\ \ f^{(K)} : \mathbb{R}^n \times \mathbb{R}^p \to \mathbb{R}^n, \tag{5}$$

where $f^{(K)}(x,\alpha)$ is K-th -th iterate of f. The study of (4) usually starts with the analysis of fixed points. Numerically we continue fixed points of this map, i.e. solutions to the equation

$$F(x,\alpha) \equiv f(x,\alpha) - x = 0. \tag{5}$$

with one control parameter. While varying one parameter, one may encounter codimension 1 bifurcations of fixed points, i.e., critical parameter values where stability of the fixed point changes. The eigenvalues of the Jacobian matrix $A = f_x$ of f are called multipliers. The fixed point is asymptotically stable if $|\mu| < 1$ for every multiplier μ. If there exists a multiplier μ with $|\mu| > 1$, then the fixed point is unstable. While following a curve of fixed points, three co-dimension 1 singularities generically occur, namely a limit point (fold, LP) with a multiplier +1, a period-doubling (flip, PD) point with a multiplier −1 and a Neimark-Sacker (NS) point with a conjugate pair of complex multipliers $\exp(\pm i\theta_0)$, $0 < \theta_0 < \pi$. Encountering such a bifurcation one may use the formulas for the normal form coefficients derived via the center manifold reduction, see e.g. (Kuznetsov, 2004), §5.4, to analysis the bifurcation. Generically, the curve of fixed points turns at an LP. In a PD point, generically, a cycle of period two bifurcates from the fixed point of f that changes stability. This bifurcation can be supercritical or subcritical, denoting the appearance of stable or unstable cycles for parameter values larger or smaller than the critical one, respectively.

When two control parameters are allowed to vary, eleven co-dimension 2 bifurcations can be met in generic families of maps (4), where curves of codimension 1 bifurcations intersect or meet tangentially. We proceed through listing smooth normal forms of only those codim 2 bifurcation points which our analysis is mainly focused on, namely, the resonant 2, 3, and 4 points. The critical

normal form coefficients for all generic codim 2 bifurcation points have been derived earlier in (Kuznetsov and Meijer, 2005; Kuznetsov and Meijer, 2006) using a combined reduction-normalization technique. This information could be used to approximate codim 1 bifurcation curves that emanate from the codim 2 points.

2.1. Normal forms of codim-1 cases

Assuming sufficient smoothness of g, we write its Taylor expansion about (x_0, α_0) as

$$\begin{aligned} g(x_0+x,\alpha_0+\alpha) &= x_0 + Ax + \tfrac{1}{2}B(x,x) + \tfrac{1}{6}C(x,x,x) \\ &+ \tfrac{1}{24}D(x,x,x,x) + \tfrac{1}{120}E(x,x,x,x,x) \\ &+ J_1\alpha + \tfrac{1}{2}J_2(\alpha,\alpha) \\ &+ A_1(x,\alpha) + \tfrac{1}{2}B_1(x,x,\alpha) + \tfrac{1}{6}C_1(x,x,x,\alpha) \\ &+ \tfrac{1}{2}A_2(x,\alpha,\alpha) + \tfrac{1}{4}B_2(x,x,\alpha,\alpha) + \tfrac{1}{12}C_2(x,x,x,\alpha,\alpha) \\ &+ \cdots, \end{aligned} \tag{7}$$

where all functions are multilinear forms of their arguments and the dots denote higher order terms in x and α. In particular, $A = g_x(x_0, \alpha)$ and the components of the multilinear functions B and C are given by

$$\begin{aligned} B_i(x,y) &= \sum_{j,k=1}^{n} \frac{\partial^2 g_i(x_0,\alpha_0)}{\partial\xi_j \partial\xi_k} x_j y_k, \; C_i(x,y,z) \\ &= \sum_{j,k,l=1}^{n} \frac{\partial^3 g_i(x_0,\alpha_0)}{\partial\xi_j \partial\xi_k \partial\xi_l} x_j y_k z_l, \end{aligned} \tag{8}$$

for $i = 1, 2, \ldots, n$. From now on, I_n is the unit $n \times n$ matrix and $\|x\| = \sqrt{\langle x, x \rangle}$, where $\langle u, v \rangle = u^T v$ is the standard scalar product in $\mathbb{C}^n$ (or $\mathbb{R}^n$).

Table 1. Smooth normal forms for generic codim 1 bifurcations of fixed points on center manifolds

	Eigenvectors	Normal form	Critical coefficients
LP	$Aq = q$ $A^T p = p$	$w \mapsto \beta + w + aw^2$ $+O(w^3), w \in \mathbb{R}$	$a = \frac{1}{2}\langle p, B(q,q)\rangle$
PD	$Aq = -q$ $A^T p = -p$	$w \mapsto -1(1+\beta)w + bw^3$ $+O(w^4), w \in \mathbb{R}$	$b = 6\langle p, C(q,q,q) + 3B(q,h_{200}$ $h_{2000} = (I_n - A)^{-1}B(q,q)$
NS	$Aq = e^{i\theta_0}q$ $A^T p = e^{i\theta_0}p$ $e^{i\nu\theta_0} \neq 1$ $\nu = 1,2,3,4.$	$w \mapsto we^{i\theta}(1+\beta+d \mid w \mid^2$ $+O(\mid w \mid^4), w \in \mathbb{C}$	$d = \frac{1}{2}e^{i\theta_0}\langle p, C(q,q,\overline{q})$ $+ 2B(q,h_{1100})$ $+ B(\overline{q},h_{2000})$ $h_{1100} = (I_n - A)^{-1}B(q,\overline{q})$ $h_{2000} = (e^{2i\theta_0}I_n - A)^{-1}B(q,q)$

2.2. Normal forms of codim-2 cases

Below we give normal forms to which the restriction of a generic map $g(x, \alpha) = f^{(K)}(x, \alpha)$ to the eleven codim 2 bifurcations of cycles that can be met in generic two-parameter families of maps are listed in Table 2.

Below we give normal forms to which the restriction of a generic map $g(x, \alpha) = f^{(K)}(x, \alpha)$ to the parameter-dependent center manifold can be transformed near the corresponding bifurcation by smooth invertible coordinate and parameter transformations. We refer to (Kuznetsov, 2004), Ch. 9, and (Kuznetsov and Meijer, 2005; Kuznetsov and Meijer, 2006) for details, including explicit expressions for all critical normal form coefficients. If a complex critical eigenvalue λ is involved, it is always assumed that $\lambda^\nu \neq 1$ for $\nu = 1,2,3,4$.

1.2. resonances (R2) Near a 1:2 resonance the restriction of the map g to the parameter-dependent center manifold is smoothly equivalent to the normal form

$$\begin{aligned} \begin{pmatrix} w_1 \\ w_2 \end{pmatrix} \mapsto \begin{pmatrix} -w_1 + w_2 \\ \beta_1 w_1 + (-1+\beta_2) + C_1(\beta)w_1^3 + D_1(\beta)w_1^2 w_2 \end{pmatrix} \\ + O(\|w\|^4), \quad w \in \mathbb{R}^2. \end{aligned} \tag{9}$$

Table 2. Generic codim 2 bifurcations of cycles

	Name	Bifurcation conditions
CP	cusp	$\lambda_1 = 1, a = 0$
DPD	degenerate flip	$\lambda_1 = -1, b = 0$
CH	Chenciner bifurcation	$\lambda_{1,2} = e^{\pm i\theta_0}, c = 0$
R1	1:1 resonance	$\lambda_1 = \lambda_2 = 1$
R2	1:2 resonance	$\lambda_1 = \lambda_2 = -1$
R3	1:3 resonance	$\lambda_{1,2} = e^{\pm i\theta_0}, \theta_0 = \frac{2\pi}{3}$
R4	1:4 resonance	$\lambda_{1,2} = e^{\pm i\theta_0}, \theta_0 = \frac{\pi}{2}$
LPPD	fold-flip	$\lambda_1 = 1, \lambda_2 = -1$
LPNS	fold-NS	$\lambda_1 = 1, \lambda_{2,3} = e^{\pm i\theta_0}$
PDNS	flip-NS	$\lambda_1 = -1, \lambda_{2,3} = e^{\pm i\theta_0}$
NSNS	double NS	$\lambda_{1,2} = e^{\pm i\theta_0}, \lambda_{3,4} = e^{\pm i\theta_1}$

that depends on two control parameters (β_1, β_2). If $C_1 < 0$, then there is a Neimark-Sacker curve of fixed points of g with double period that emanates from the flip bifurcation curve $\beta_2 = 0$ of fixed points. There are also global bifurcations associated with the destruction of closed invariant curves. The critical normal form coefficients are $[c, d] = [4C_1(0), -6C_1(0) - 2D_1(0)]$. The signs of these coefficients determine the dynamic behavior of the map near the R2 point. For example, if they are both negative, then we have the situation of (Kuznetsov, 2004), (case $s = -1$) and there is a region of parameter values near the R2 point where an unstable 2-cycle coexists with a stable closed invariant curve.

1.3. resonance (R3) At a 1:3 resonance, the restriction of the map g to the parameter-dependent center manifold is smoothly equivalent to the normal form

$$z \mapsto (\mathrm{e}^{2i\pi/3} + \beta)z + B_1\bar{z}^2 + C_1 z\,|\,z\,|^2 + \mathrm{O}(|\,z\,|^4),\quad z \in \mathbb{C}. \quad (10)$$

A generic unfolding of this singularity has a period-3 saddle cycle that does not bifurcate for nearby parameter values, although it merges with the primary fixed point as the parameters approach R3. The critical normal form coefficient is $\Re(c_1)$ where $c_1 = \exp(\frac{i4\pi}{3})C_1 - |\,B_1\,|^2$. The sign of $\Re(c_1)$ determines the dynamic behavior of the map near the R3 point. If it is negative (positive) then there is a region near the R3 point where a stable (respectively, unstable) invariant closed curve coexists with an unstable (respectively, stable) equilibrium. In all non-degenerate cases unstable 3-cycles exist near the R3 point and in many applications these gain stability through further fold bifurcations.

1.4. resonance (R4) Near a 1:4 resonance the restriction of the map g to the parameter-dependent center manifold is smoothly equivalent to the normal form

$$z \mapsto (i + \beta)z + C_1(\beta)z^2\bar{z} + D_1(\beta)\bar{z}^3 + \mathrm{O}(|\,z\,|^4),\quad z \in \mathbb{C}. \quad (11)$$

The critical (complex) normal form coefficient is $A = -iC_1(0)/\,|\,D_1(0)\,|$. It determines the dynamic behavior of the map near the R4 point. In particular, if $\|A\| > 1$ then stable 4-cycles exist in a region near the R4 point and two half-lines of fold bifurcations of 4-cycles emanate from the R4 point.

3. Fixed points of the system and their stability

We start the bifurcation analysis of (3) with fixed points, which are the solutions to

$$x^* + \delta(rx^*(1-x^*) - bx^*y^*) = x^*,\ y^* + \delta(-d + bx^*)y^* = y^*.$$

The origin F1 = (0, 0) is a fixed point of (3) but is of little interest. Two further fixed points of the system are given by $F_2 = (1,0)$ and $F_3 = (\frac{d}{b}, \frac{r(b-d)}{b^2})$. We note that F_3 is biologically possible only if its coordinates are nonnegative, i.e. $b \geq d$.

We start the local bifurcation analysis of the map (3) by linearization of F around each of its fixed points. The Jacobian matrix $J(x,y)$ is given by:

$$J(x,y) = \begin{bmatrix} 1 + r\delta - 2r\delta x - b\delta y & -b\delta x \\ b\delta y & 1 - d\delta + b\delta x \end{bmatrix}. \quad (12)$$

The characteristic equation of $J(x,y)$ is given by

$$\lambda^2 - tr(J) + det(J) = 0, \quad (6)$$

where

$$tr(J) = -2 + d\delta - r\delta + (2r\delta - b\delta)x + by\delta,$$

and

$$det(J) = b2\delta 2xy + (1 + r\delta - 2r\delta x - b\delta y)(1 - d\delta + b\delta x).$$

3.1. Stability of F_1

Proposition 1. The fixed point F_1 is unstable for all admissible parameter sets
(i.e. with positive parameters).

Proof: Eigenvalues of the Jacobian at F_1 are $\lambda_1 = 1 + r\delta$ and $\lambda_2 = 1 - d\delta$. For all feasible values of r and δ, $\lambda_1 > 1$, i.e. F_1 is unstable.

3.2. Stability of F_2

The Jacobian matrix of (3) at F_2 is given by

$$J(F_2) = \begin{pmatrix} 1 - r\delta & -b\delta \\ 0 & 1 - d\delta + b\delta \end{pmatrix}. \quad (7)$$

The multipliers $J(F_2)$ are $\lambda_1 = 1 - r\delta$ and $\lambda_2 = 1 + \delta(b-d)$.

Proposition 2. The fixed point F_2 is asymptotically stable if and only if $\frac{d}{b} > 2$ and $0 < \delta < \min\left\{\frac{2}{d-b}, \frac{2}{r}\right\}$. Moreover, it loses stability:
(i) via a supercritical flip for $\delta = \frac{2}{r}$ and $\delta = \frac{2}{d-b}$.
(ii) via branching for $b = d \neq 0$ and there bifurcates to F_3.

Proof: F_2 is asymptotically stable if and only if $|\lambda_1| < 1$ and $|\lambda_2| < 1$. These imply $0 < \delta < \frac{2}{r}$ and $0 < \delta < \frac{2}{d-b}$.
Let $\delta = \frac{2}{r}$ then $\lambda_1 = 1 - r\delta = -1$ which correspond to a PD point. For super criticality of the period doubling point it is sufficient to show that the corresponding critical normal form coefficient b, given in Table 1, is positive. Here $A = J(F_2)$, $B(.,.)$ and $C(.,.,.)$ are the second and third order multilinear forms respectively, p and q are the left and right eigenvectors of A for the eigenvalue −1, respectively. These vectors are normalized by $\langle p, q \rangle = 1$, $\langle q, q \rangle = 1$, where $\langle .. \rangle$ is the standard scalar product in $\mathbb{R}^2$. We obtain:

$$q = \begin{pmatrix} q_1 \\ q_2 \end{pmatrix} = \begin{pmatrix} 1 \\ 0 \end{pmatrix} \quad (8)$$

and

$$p = \begin{pmatrix} p_1 \\ p_2 \end{pmatrix} = \begin{pmatrix} 1 \\ 1 - \frac{d}{b} \end{pmatrix} \quad (9)$$

The components of the multilinear form $B(q,q)$ are given by:

$$[B(q,q)]_1 = \sum_{j,k=1}^{2} \frac{\partial^2(x + \delta(rx(1-x) - bxy)y + \delta(-d + bx)y)}{\partial x_j \partial x_k} q_j q_k = -2\delta r \quad (17)$$

$$[B(q,q)]_2 = \sum_{j,k=1}^{2} \frac{\partial^2(y + \delta(-d + bx)y)}{\partial x_j \partial x_k} q_j q_k = 0, \quad (18)$$

where the state variable vector is for ease of notation generically denoted by $(x_1, x_2)^T$ instead of $(x, y)^T$.

Let $\zeta = (I - A)^{-1} B(q,q)$, then we have $\zeta = \begin{pmatrix} -1 \\ 0 \end{pmatrix}$ and find

$$\left[B\left(q,\zeta\right)\right]_1 = 4\delta r,\ \left[B\left(q,\zeta\right)\right]_2 = 0. \quad (10)$$

The third order multilinear form $C\left(q,q,q\right)$ is given by

$$[C(q,q,q)]_1 = \sum_{j,k,l=1}^{2} \frac{\partial^3 (x + \delta(rx(1-x) - bxy))}{\partial x_j \partial x_k \partial x_l} q_j q_k q_l = 0. \quad (11)$$

$$[C(q,q,q)]_2 = \sum_{j,k,l=1}^{2} \frac{\partial^3 (y + \delta(-d + bx)y)}{\partial x_j \partial x_k \partial x_l} q_j q_k q_l = 0. \quad (12)$$

The critical normal form coefficient b is given by

$$b = \frac{1}{6} p^T \begin{pmatrix} 12\delta r \\ 0 \end{pmatrix} = 2\delta r = 4. \quad (13)$$

which is clearly positive. This completes the proof of supercriticality of the flip point at F_2.

In the case of $\delta = \frac{2}{d-b}$, we obtain the right eigenvector

$$q = \begin{pmatrix} q_1 \\ q_2 \end{pmatrix} = \begin{pmatrix} 1 \\ 0 \end{pmatrix}. \quad (14)$$

and the left eigenvector

$$p = \begin{pmatrix} p_1 \\ p_2 \end{pmatrix} = \begin{pmatrix} 1 \\ \dfrac{d-b-r}{b} \end{pmatrix}. \quad (15)$$

To prove the supercriticality of the PD point in this case we use the same procedure as in the case where $\delta = \frac{2}{r}$. We obtain the normal form coefficient $b = \frac{4r}{d-b}$ which is clearly positive since $d > b$ (otherwise $\delta = \frac{2}{d-b} < 0$, which is not biologically feasible).

If $r = d \neq 0$ then the coordinates of F_3 are $\frac{d}{b} = 1$ and $\frac{r(b-d)}{b^2} = 0$, the point $(1,0)$ becomes an intersection point of the two branches of F_2 and F_3.

3.3. Stability and bifurcation of F3

To study the stability of F_3 we use the Jury's criteria, see (Murray, 1993), §A2. 1. Let $F(\lambda) = \lambda^2 - tr(J(F_3))\lambda + \det(J(F_3))$ be the characteristic equation of $J(F_3)$. Hence we have $F(\lambda) = (\lambda - \lambda_1)(\lambda - \lambda_2)$ where λ_1 and λ_2 are the eigenvalues of $J(F_3)$. According to the Jury's criteria F_3 is asymptotically stable if the following conditions hold:

$$\begin{aligned} &F(-1) = 1 + tr(J(F_3)) + \det(J(F_3)) > 0, \\ &F(1) = 1 - tr(J(F_3)) + \det(J(F_3)) > 0, \\ &1 - \det(J(F_3)) > 0. \end{aligned} \quad (16)$$

Proposition 3. Suppose $b > d$ then F_3 is asymptotically stable if and only if one of the following mutually exclusive conditions holds:

(i) $r \geq \dfrac{4b(b-d)}{d}$

and $0 < \delta < \dfrac{rd - \sqrt{rd(rd - 4b(b-d))}}{rd(b-d)}$,

(ii) $0 < r < \dfrac{4b(b-d)}{d}$ and $0 < \delta < \dfrac{1}{b-d}$.

Proof: At F_3 we have:

$$J(F_3) = \begin{bmatrix} 1 + r\delta - 2rd\frac{\delta}{b} - \frac{1}{b}\delta r(b-d) & -\delta d \\ \frac{1}{b}\delta r(b-d) & 1 \end{bmatrix}. \quad (17)$$

Then we get:

$$tr(J(F_3)) = 2 - r\delta\frac{d}{b},\ det(J(F_3)) = 1 - \frac{r\delta d}{b}(1 + \delta(d-b)),$$

The criterion $F(1) > 0$ is easily seen to be equivalent to the condition $r\delta^2 d(b-d) > 0$.

This condition holds when $b > d$, i.e., the condition under which F_3 is biologically possible.

The criterion $1 - \det(J(F_3)) > 0$ is easily seen to be equivalent to the condition

$$\delta < \frac{1}{b-d}. \quad (27)$$

The criterion $F(-1) > 0$ is easily seen to be equivalent to the condition $r\delta^2 d(b-d) - 2r\delta d + 4b > 0$. Roots of this quadratic equation in δ are:

$$\delta_{1,2} = \frac{rd \pm \sqrt{rd(rd - 4b(b-d))}}{rd(b-d)}. \quad (28)$$

If $rd(rd - 4b(b-d)) > 0$, equivalently $r \geq \frac{4b(b-d)}{d}$, then F_3 is stable when $0 < \delta < \frac{rd - \sqrt{rd(rd-4b(b-d))}}{rd(b-d)}$. Otherwise, if $rd(rd - 4b(b-d)) > 0$ then F_3 is stable when $0 < \delta < \frac{1}{b-d}$.

Proposition 4. F_3 loses stability:

(i) via a flip point when $r \geq \frac{4b(b-d)}{d}$ and $\delta = \frac{rd - \sqrt{rd(rd-4b(b-d))}}{rd(b-d)}$.

(ii) via a Neimark-Sacker point when $0 < r < \frac{4b(b-d)}{d}$ and $\delta = \frac{1}{b-d}$

(iii) via a branch point when $b = d$ and there bifurcates to F_2.

Proof: By Proposition 3 the stability boundaries of F_3 consist of parts of three curves, namely

Curve 1. $\delta = \frac{rd - \sqrt{rd(rd-4b(b-d))}}{rd(b-d)}$,

Curve 2. $\delta = \frac{1}{b-d}$,

Curve 3. $b = d$.

The points of Curve 1 which are on the stability boundary of F_3 satisfy $F(-1) = 0$, i.e. they have an eigenvalue -1. The points of Curve 2 which are on the stability boundary satisfy $\det(J(F_3)) = 1$, i.e. they have two eigenvalues with product 1. The points of Curve 3 which are on the stability boundary satisfy $F(-1) = 0$, i.e., they have an eigenvalue -1.

Combining this with Proposition 2 we find that the interior points of the boundary parts of Curves 1, 2, and 3 form the sets described in parts (i), (ii) and (iii) of the Proposition, respectively.

4. Numerical bifurcation analysis of F_2 and F_3

In this section we perform a numerical bifurcation analysis by using the MATLAB package MATCONTM**,** see (Govaerts et al., 2007). The bifurcation analysis is based on continuation methods, whereby we trace solution manifolds of fixed points while some parameters of the map vary, see (Allgower and Georg, 1990).

4.1. Numerical bifurcation of F_2

By continuation of $F_2 = (1;0)$ starting from $\delta = 0.3$, $b = 0.6$, $d = 0.8$, $r = 2$ in the stable region of F_2 (stability follows from Proposition 2), with δ free, we see that F_2 is stable when $0 < \delta < 1$. It loses stability via a supercritical period doubling point (*PD*, the corresponding normal form coefficient is $4 > 0$ which confirms (22)) when $\delta = 1$, and via a neutral saddle when b crosses 0. The output of *Run 1* is given by:

label = PD, x = (1. 000000 0. 000000 1. 000000)
normal form coefficient of PD = 4. 000000e+000
label = NS, x = (1. 000000 0. 000000 -0. 000000)
Neutral saddle

We note that at PD bifurcation point $b = 1$ which agrees with Proposition 2 part (i) since $\frac{2}{r} = 1 = b$. We also remark that the detected Neutral saddle bifurcation point is indeed a resonance 1:1, R1 point which is a degenerate case where two multipliers become 1. The first two entries of x are the coordinate values of the fixed point F_2, and the last entry of x is the value of the free parameter δ at the corresponding bifurcation point. We note that the normal form coefficient of the *PD* point is 4, confirming (22).

Beyond the *PD* point the dynamics of (3) is a stable 2-cycle. MATCONTM allows a switch to the continuation of this 2-cycle. It loses stability at a supercritical *PD* point:

label = PD, x = (1. 196923 0. 000000 1. 224745)
normal form coefficient of PD = 2. 048528e+002
A stable 4-cycle is born when $\delta > 1.224745$. It loses stability via a supercritical PD point:
label = PD, x = (1. 231541 0. 000000 1. 272045)
normal form coefficient of PD = 8. 333696e+003
Thus, when $\delta > 1.272045$ a stable 8-cycle emerges. A stable 8-cycle is given by $C_8 = \{X_1^8, ..., X_8^8\}$ where $X_1^8 = (1.159799265, 0)$ where $\delta = 1.281,\ b = .6, d = .8, r = 2$ We note that for F_2 the map (3) is a logistic map. In fact, in this case the predator becomes extinct and the prey undergoes the period-doubling bifurcation to chaos through a cascade of period doublings for further increasing the parameter δ, see (Kraft, 1999).

Continuation of F_2 starting from the same parameter values as in *Run 1*, with b as free parameter, leads to:
label = BP, x = (1. 000000 0. 000000 0. 800000)
The appearance of a branch point is consistent with Proposition 2 part (ii) which states that F_2 bifurcates to F_3 when $0 \neq b = d = 0.8$.

4.2. Numerical bifurcation of F_3

By continuation of $F_3 = (0.625; 0.9375)$ which is in the stable region for parameter values $\delta = 1.3,\ b = 0.6,\ d = 0.5,\ r = 2$ with b free, we see that F_3 is stable when $0.605448 < b < 1.269231$. It loses stability via a supercritical period doubling point (PD, the corresponding normal form coefficient is $6.890328e-001 > 0$) when $b = 0.605448$ which is consistent with Proposition 4 part (i) ($\frac{rd-\sqrt{rd(rd-4b(b-d))}}{rd(b-d)} = 0.5 = \delta$), and via a supercritical Neimark-Sacker (NS bifurcation point, the corresponding normal form coefficient is $-1.685059 < 0$) when b crosses 1.269231, which is consistent with Proposition 4 part (ii) ($\frac{1}{b-d} = 1.269231 = \delta$). The output of *Run 1* is given by:
label = NS, x = (0. 393939 0. 955005 1. 269231)
normal form coefficient of NS = -1. 685059e+000
label = PD, x = (0. 825835 0. 575327 0. 605448)
normal form coefficient of PD = 6. 890328e-001
label = BP, x = (1. 000000 0. 000000 0. 500000)

The two first entries of x are the coordinate values of the fixed point F_3, and the last coordinate of x is the value of the free parameter b at the corresponding bifurcation point. The curve computed in *Run 1* is presented in Fig. 1.

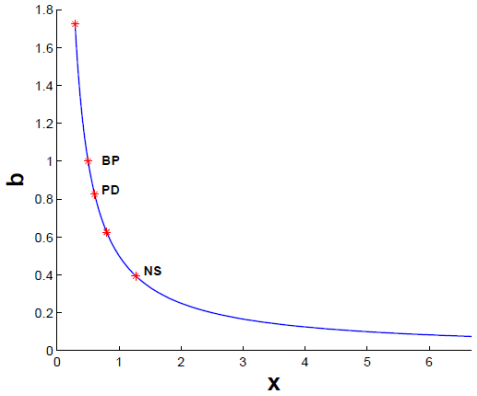

Fig. 1. Continuation of F_3 in (x, b) -space

Now we compute the period doubling curve, where δ and b are free, by starting from the *PD* point of *Run 1*. We call this *Run 2*.
label = GPD, x = (0. 736108 0. 777012 1. 583118 0. 679248).
Normal form coefficient of GPD = 4. 501959e-001
label = R2, x = (0. 618034 0. 944272 3. 236068 0. 809017).
Normal form coefficient for R2:[c, d]=4. 277832e+001, -1. 537955e+002
label = LPPD, x = (1. 000000 0. 000000 1. 000000 0. 500000)
Normal form coefficient for LPPD :[a/e, be]= -2. 000000e-001, -4. 486522e-009,
First Lyapunov coefficient for second iterate = 1. 034838e-008,
Three codim-2 bifurcation points are detected on the fold curve, namely a generalized period doubling point *GPD*, a fold-flip *LPPD* and a resonance 2 bifurcation R2. This curve is shown in Fig. 2.

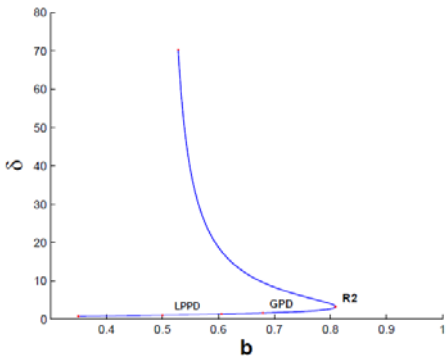

Fig. 2. Flip bifurcation curve in (b, δ) - space

Now we compute the NS curve, where b and r are free, by starting from the NS point of *Run 1*. We call this *Run 3*.
label = R4, x = (0. 393939 1. 864802 1. 269231 3. 905325 0. 000000)
Normal form coefficient of R4 : A = -8. 462220e-001 + 6. 323958e-001 i
label = R3, x = (0. 393939 2. 797203 1. 269231 5. 857988 -0. 500000)
Normal form coefficient of R3: Re(c_1) = -3. 599349e-001
label = R2, x = (0. 393939 3. 729604 1. 269231 7. 810651 -1. 000000)
Normal form coefficient of R2: [c, d] = -3. 262690e-001, -2. 432859e+001
label = R1, x = (0. 393939 0. 000000 1. 269231 -0. 000000 1. 000000)
Normal form coefficient of R1 : s = 0
label = CH, x = (0. 393939 0. 000000 1. 269231 0. 000000 1. 000000)
Normal form coefficient of CH = 5. 984655e+004
This curve is shown in Fig. 3.

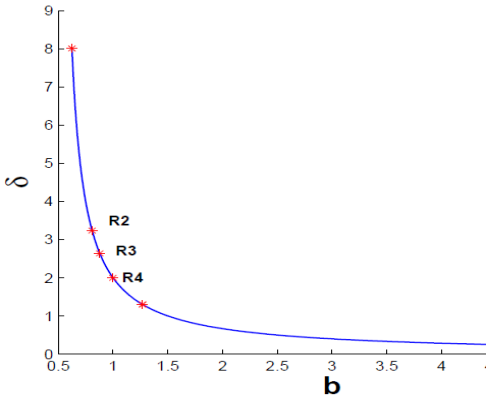

Fig. 3. Neimark-Sacker bifurcation

4.3. Orbits of higher period 3, 4, 8, 16

Since $|A|>1$ (*A* is the normal form coefficient of the $R4$ point in *Run 3*), two cycles of period 4 of the map are born. A stable 4-cycle for $\delta=2$, $b=1.000188$, $d=0.5$ and $r=2$ is given by: $C_4=\{X_1,X_2,X_3,X_4\}$ where $X_1=(0.489528,0.997275)$. We present this cycle in Fig. 4. In order to compute the stability region of this 4-cycle, we compute two fold curves of the fourth iterate rooted at the R4 point. These curves exist since $|A|>1$, see (Kuznetsov, 2004) (switching from an R4 point to the fold curves of the fourth iterate is supported by MATCONTM. The stable fixed points of the fourth iterate exist in the wedge between the two fold curves. The output of this continuation, *Run 4*, is given below.

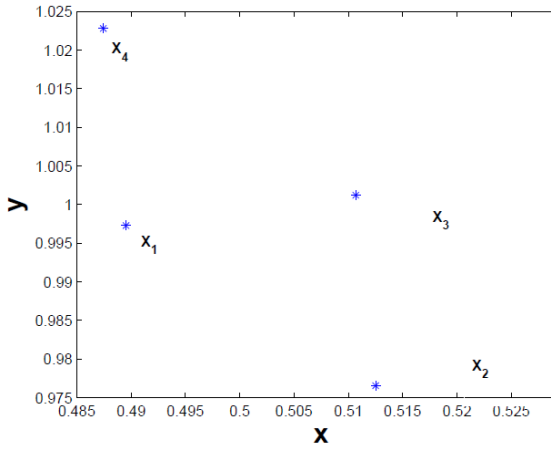

Fig. 4. stable 4-cycle for δ = 2, b = 1.000187717308457, *d* = 0.5 and *r* = 2

label = LPPD, x = (0. 673979 0. 697820 2. 163102 1. 028287)
Normal form coefficient for LPPD: [a/e, be]= 7. 085141e-001, -6. 966717e+000,
label = R1, x = (0. 198562 1. 156169 1. 714470 1. 144735)
normal form coefficient of R1 = -1
label = CP, x = (0. 070058 0. 268386 1. 591519 1. 209986)
Normal form coefficient of CP s= 1. 166728e-002
We further compute a curve of fixed points of the fourth iterate starting from the 4-cycle C_4 represented in Fig. 4 with control parameter b. The curve is shown in Fig. 5.

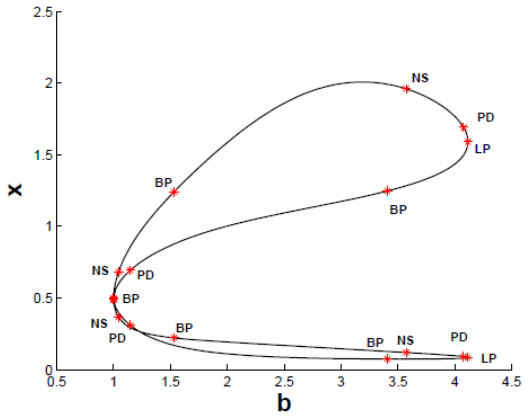

Fig. 5. Curve of fixed points of the fourth iterate starting from the 4-cycle C_4

The 4-cycle is stable in the wedge between two LP^4 curves, and loses stability via the supercritical Neimark-Sacker bifurcation point corresponding to $b=1.043316$. Now we compute a NS-curve starting from this NS

bifurcation point with control parameters δ and b in *Run 5* given below.
label = R4, x = (0. 351278 0. 785983 1. 907838 1. 059669 0. 000000)
Normal form coefficient of R4: A=-4. 940734e+000 + -2. 267963e+000 i
label = R1, x = (0. 293667 0. 615620 1. 714470 1. 144735 1. 000000)
Normal form coefficient of R1: s = -1
label = R3, x = (0. 368126 0. 806437 2. 055728 1. 039985 -0. 500000)
Normal form coefficient of R3: Re(c_1) = -1. 386428e+001
label = R2, x = (0. 364147 0. 790371 2. 160913 1. 043191 -1. 000000)
Normal form coefficient of R2: [c, d] = -7. 104480e+000, -4. 372905e+002

We consider the R4 bifurcation point in *Run 5*, since $|A|>1$ (A is the normal form coefficient of the $R4$), two cycles of period 16 of the map are born. A stable 16-cycle for $\delta=1.928$, $b=1.059$, $d=0.5$ and $r=2$ is given by:

$$C_{16}=\left\{X_1^{16},X_2^{16},X_3^{16},...,X_{16}^{16}\right\}$$

where

$$X_1^{16}=(0.711719566255687,0.544588658381816)$$

for $\delta=1.928$, $b=1.059$, $d=0.5$ and $r=2$. We present this cycle in Fig. 6.

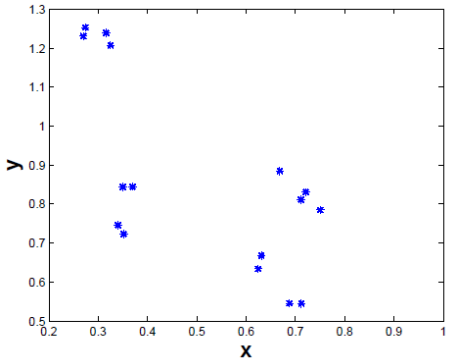

Fig. 6. Stable 16-cycle for $\delta=1.928$, $b=1.059$, $d=0.5$ and $r=2$

In order to compute the stability region of this 16-cycle, we compute two-fold curves of the sixteenth iterate rooted at the $R4$ point. The stable fixed points of the sixteenth iterate exist in the wedge between the two-fold curves. The output of this continuation**,** *Run 6***,** is given below. The curves are shown in Fig. 7 and indicated by LP^{16} curves.
label = LPPD, x = (0. 372145 0. 876627 2. 099357 1. 047459)

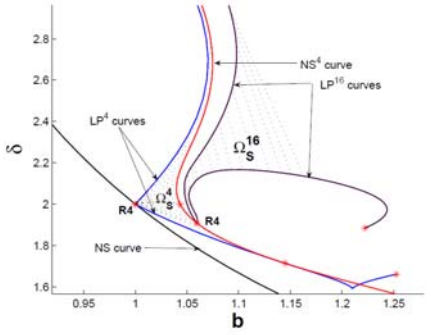

Fig. 7. Bifurcation curves of *NS*, *NS*^{4}, two curves of *LP*^{4} emanating at the R_4, and two curves of LP16 emanating at the R_4 of the fourth iterate of (3). These curves form stability boundaries of 4-cycle Ω_S^4 and 16-cycle (Ω_S^{16})

Normal form coefficient for LPPD: [a/e, be]= 1. 655004e+001, 5. 026210e+002,
First Lyapunov coefficient for second iterate = 5. 026210e+002,
label = LPPD, x = (0. 403179 0. 917839 2. 019839 1. 052334)
Normal form coefficient for LPPD: [a/e, be]= 2. 752071e-001, 2. 068768e+002,
First Lyapunov coefficient for second iterate = 2. 068768e+002,
label = R1, x = (0. 335845 1. 008983 2. 123921 1. 175213)
normal form coefficient of R1 = -1
label = LPPD, x = (0. 335860 1. 009023 2. 123965 1. 175170)
Normal form coefficient for LPPD: [a/e, be]= -5. 031350e-001, -4. 743114e+012,

Next we consider the resonance 1:3 point in *Run 3*. Since its normal form coefficient is negative, the bifurcation picture near the R3 point is qualitatively the same as presented in (Kuznestov, 2004), Fig. 8. In particular, there is a region near the R3 point where a stable invariant closed curve coexists with an unstable fixed point. For parameter values close to the $R3$ point, the map has a saddle cycle of period three.

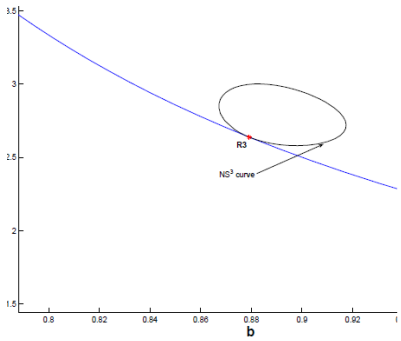

Fig. 8. A curve of Neutral Saddle points of the third iterate emanates from an *R*3 point

Furthermore, a neutral saddle bifurcation curve of fixed points of the third iterate emanates (Kuznetsov, 2004), Ch. 9. We compute this curve by branch switching at the R3 point. This curve is presented in Fig. 9. Now we consider the GPD point computed in *Run 2*. We compute a branch of fold points of the second iterate by switching at the GPD point. This curve emanates tangentially to the PD curve and forms the stability boundary of the 2-cycles which are born when crossing the PD curve. The output of this continuation, *Run 5*, is given below. This curve is superposed on Fig. 2 and presented in Fig. 9.

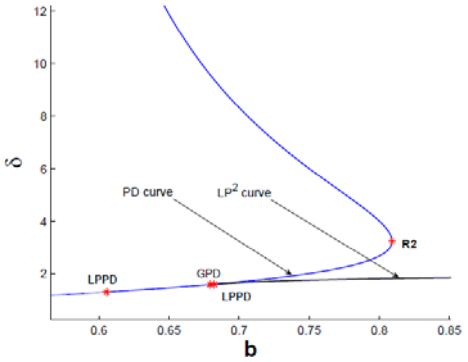

Fig. 9. A curve of fold bifurcations of the second iterate, LP2, which emanates tangentially at a GPD point on a flip curve

label = LPPD, x = (0. 551673 0. 636994 1. 596160 0. 682279)
Normal form coefficient for LPPD: [a/e, be]= 5. 849246e-004, 6. 672972e+000,

4.4. Computation of Arnol'd tongues

We consider the expansion (7) for small $|x|$. Then, generically, for any rational $q = \frac{m}{n}$ with coprime positive integer m and n there exists an open connected set Ω_q called the Arnold tongue, see (Lauwerier, 1986), with $\lambda_q = e^{2\pi qi} \in \overline{\Omega}$ such that map (4) has a periodic point of the period n whenever the Jacobian matrix *A* has an eigenvalue μ_λ in Ω_q and the norms of the n-periodic points tend to zero as μ_λ tends to λ_q along the set Ω_q (see, e.g. (Arnold, 1995). Rational number $q = \frac{m}{n}$ corresponds to a periodic orbit of period n such that the iterations visit all the periodic points, every m turns around the fixed point, see (Guckenheimer, 1985). The values $q = \frac{m}{n}$ with $n = 1,2,3,4$ are called strong resonances.

It is well known that near a Neimark-Sacker curve there exists a dense array of resonance tongues, generalizing the isolated tongue of period 4 in Fig. 7. The tongues locally form an open and dense set of the parameter plane. There are also quasi-periodic invariant circles in between that correspond to a set of positive measure in the parameter plane. So far, no numerical methods have been implemented to specifically compute the boundaries of the resonance tongues that are rooted in weakly resonant Neimark-Sacker points (unlike the strong resonant 1:4 case). However, since they are limit point curves of fixed points of cycles with known periods, they can be computed relatively easily if the cycles inside the tongue are globally stable (which depends on the criticality of the Neimark-Sacker curve and the noncritical multipliers as well). It is sufficient to find a fixed point of cycles inside the tongue by orbit convergence and to continue it in one free parameter to find a point on the boundary of the Arnol'd tongue as a limit point of cycles. From this, the boundary curves can be computed by a continuation in two free parameters. Its computation started from a stable 5-cycle with $x = 0.603876$; $y = 0.955237$, $a = 12.7$, $b = 3$ $\delta = 3.014$, $b = 0.832$, $d = .5$ and $r = 2$. We note that the boundary curves contain further bifurcation points. From the ecological point of view, this means that we have described a parameter region where predator and prey can coexist in a stable way and reproduce their densities every fifth year.

5. Numerical simulation

To reveal the qualitative dynamical behaviors of (1) near the NS point, in *Run 1*, we present a complete bifurcation sequence that is observed for different values of b. We fix the parameters $\delta = 1.3$, $b = 0.6$, $d = 0.5$, $r = 2$ and consider several values of b.

Figure 10 shows that F_3 is a stable attractor for $b = 1.26$. The behavior of (1) before the NS point at $b = 1.26$ is depicted in Fig. 11.

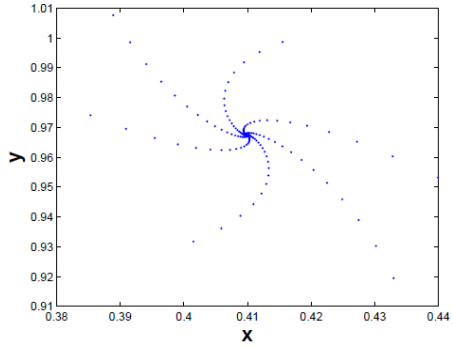

Fig. 10. An attracting fixed point for system (3) which exists for $b = 1.25$

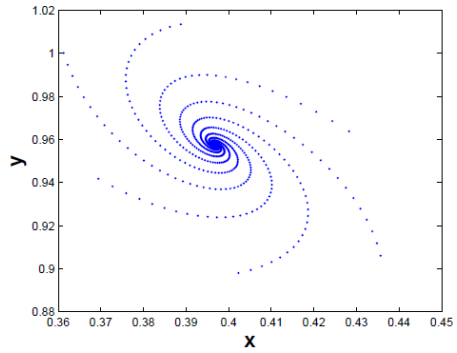

Fig. 11. Phase portrait for the system (3) which exists for $b = 1.26$

Figure 12 demonstrates the behavior of the model after the NS bifurcation when $b = 1.2696$. From Fig. 11 and Fig. 12 it turns out that the fixed point F_3 loses its stability through a NS bifurcation, when b varies from 1.26 to 1.2696. Since the critical normal form coefficient corresponding to the NS point is negative, then a stable closed invariant curve bifurcate from F_3 which coexists with unstable fixed point F_3. Figure 13 demonstrates and confirms the above statement.

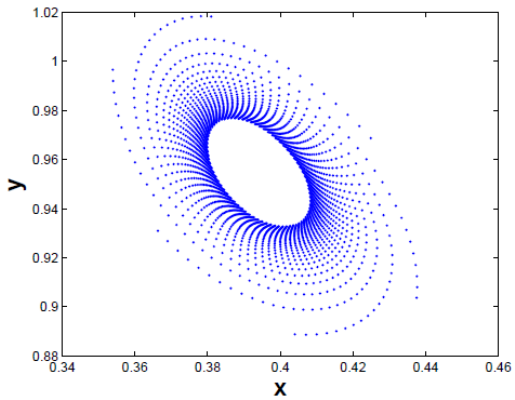

Fig. 12. Phase portrait for the system(3) for $b = 1.2696$.

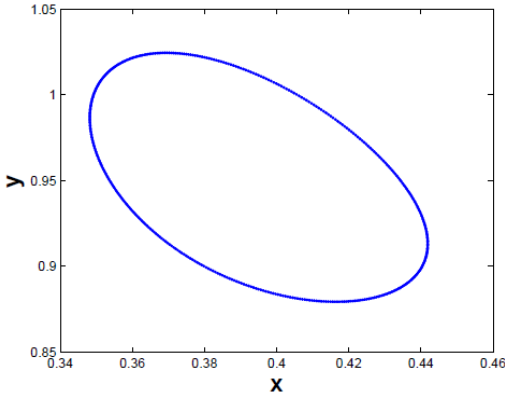

Fig. 13. A stable closed invariant curve for the system (3) for $b = 1.2696$

As b is increased further, however, the phase portrait starts to fold. We see that the circle, after being stretched, shrunk and folded creates new phenomena due to the breakdown of the closed curve, Fig. 14. For further increasing b we obtain the multiple invariant closed curves brought about by the NS bifurcation point of iterates of (1). In these cases higher bifurcations of the torus occurs as the system moves out of quasi-periodic region by increasing b. The dynamics move from one closed curve to another periodically, but the dynamics in each closed curve, may be periodic or quasi-periodic. Figure 15 presents the set of closed curves around the NS bifurcation.

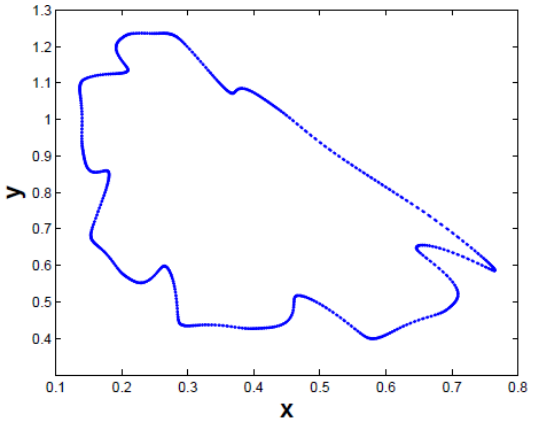

Fig. 14. The breakdown of the closed invariant curve of the system (3) for $b = 1.49$

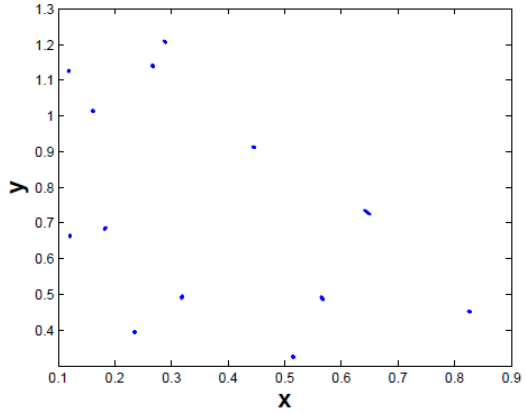

Fig. 15. The existence of multiple closed curves of the system (3) for $b = 1.553$

The radius of quasi-periodic solution grows as b is further increased as shown in Fig. 16.

Moreover, the closed curves may break leading to multiple fractal tori on which the dynamics of (1) are chaotic. Figures 17 and 18 present strange attractors for (1) with $b = 1.55$ and $b = 1.75$ respectively, which exhibit fractal structure.

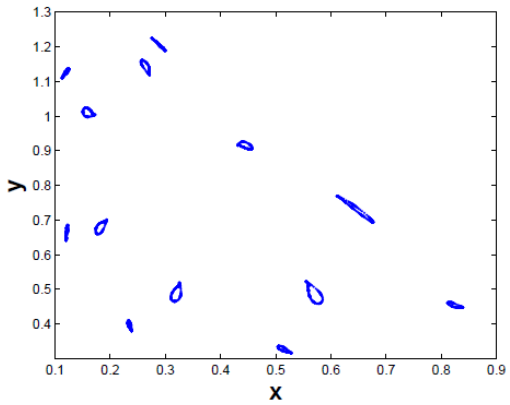

Fig. 16. A set of multiple closed curves of the system (3) for $b = 1.554$

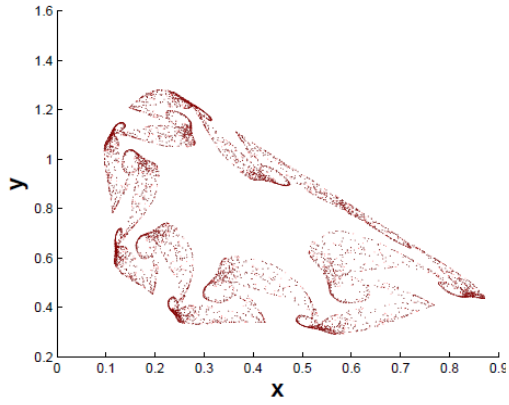

Fig. 17. Chaotic attractor for the system (3) which exists for $b = 1.556$

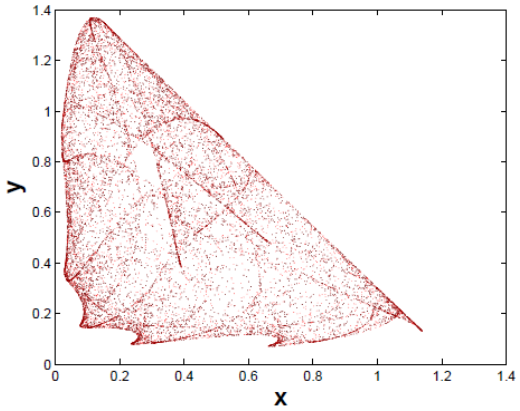

Fig. 18. Chaotic attractor for the system (3) which exists for $b = 1.75$

6. Concluding remarks

We investigated the dynamical behavior of a discrete-time Lotka-Volttera system. In Section 3, we focused on the stability and possible bifurcations of three types of fixed points of the model denoted F_1, F_2 and F_3 respectively. We established the stability condition and branching behavior of F_1 in Proposition 1. Conditions under which F_2 may bifurcate to a flip or a branch point, are derived in Proposition 2. We proved supercriticality of the flip bifurcations of F_2 by computing the corresponding normal form coefficient. Proposition 3 provides the necessary and sufficient conditions under which F_3 is stable. All possible bifurcations of F_3 are given in Proposition 4. In Section 4, we computed curves of fixed points and codim 1 bifurcations of cycles. In particular, we computed curves of fold and Neimark-Sacker bifurcations of the fourth iterate. These curves bound the stability region of an 4-cycle that is born when a fixed point of the fourth iterate crosses a supercritical Neimark-Sacker point. Furthermore, curves of fold points of the sixteenth iterate are computed which bound the stability region of a 16-cycle that appears near a resonance 4 point of the fourth iterate. We have shown that a system modeled by map (3) may exhibits quasiperiodic motion beginning from a supercritical NS bifurcation of a stable fixed point inside an Arnol'd tongue. We have shown that as one moves away from the NS bifurcation point of Fig. 1, the invariant closed curves which have initially elliptic form, increases until it begins to be deformed (see Fig. 14). The deformed curves folds more and more

on itself until, far away from the NS curve, the chaotic state is reached (see Fig. 18 and Fig. 19).

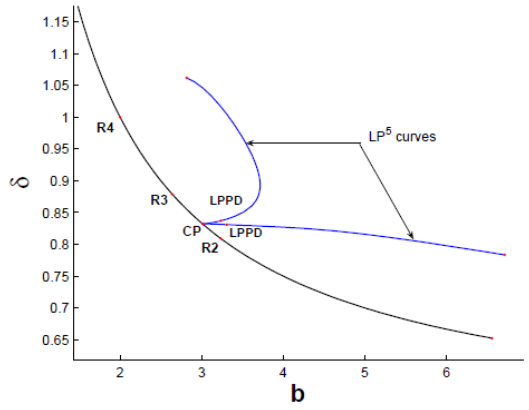

Fig. 19. An Arnol'd tongue rooted in a weak 2:5 resonant Neimark- Sacker point

Acknowledgments

The author would like to thank Shahrekod University for the financial support of this work through a research grant. The author was also partially supported by the Center of Excellence for Mathematics, Shahrekord University.

References

Agarwal, R. P. (2000). *Difference Equations and Inequalities*. Marcel Dekker, New York.

Agiza, H. N., Elabbasy, E. M., El-Metwally, H., & Elsadany, A. A. (2009). Chaotic dynamics of a discrete preypredator model with Holling type II. *Nonlinear Analysis: Real World Aplications,* 10, 116–129.

Allgower, E. L., & Georg, K. (1990). *Numerical Continuation Methods: An Introduction*. Springer-Verlag.

Arnold, V. I. (1995). *Mathematical Methods of Classical Mechanics*. Translated from the 1974 Russian original by K. Vogtmann and A. Weinstein. Corrected reprint of the second (1989) edition, Graduate Texts in Mathematics, 60. Springer, New York.

Beddington, J. R., Free, C. A., & Lawton, J. H. (1975). Dynamic complexity in predator-prey models framed in difference equations. *Nature*, doi: 10.1038/255058a0.

Blackmore, D., Chen, J., Perez, J., & Savescu, M. (2001). Dynamical properties of discrete Lotka-Volterra equations. *Chaos Solitons Fractals*, 12(13), 2553–2568.

Brauer, F., & Castillo-Chavez, C. (2001). *Mathematical models in population biology and epidemiology*. New York: Springer-Verlag.

Cai, Z., & Huang, L. (2013). Periodic dynamics of delayed Lotka-Volterra competition systems with discontinuous harvesting policies via differential inclusions, *Chaos, Soli-tons and Fractals*, doi:10.1016/j.chaos.2013.05.005.

Danca, M., Codreanu, S., & Bako, B. (1997). Detailed analysis of a nonlinear prey-predator model. *Journal of biological physics*, 23(1), 11–20.

Dawes J. H. P., & Souza, M. O. (2013). A derivation of Holling's type I, II and III functional responses in predator-prey systems. *Journal of Theoretical Biology*, doi: 10.1016/j.jtbi.2013.02.017.

Freedman, H. I., & Mathsen, R. M. (1993). Persistence in predator-prey systems with ratio-dependent predator influence, Bulletin of Mathematical Biology. 55(4) 817–827.

Freedman, H. I. (1980). *Deterministic Mathematical Models in Population Ecology*. Marcel Dekker, New York.

Govaerts, W., Khoshsiar Ghaziani, R., Kuznetsov, Yu. A., & Meijer, H. G. E. (2007). Numerical Methods for Two-Parameter Local Bifurcation Analysis of Maps. *Siam Journal* on *Scientific Computing*, 29(6), 2644–2667.

Goh, B. S. (1980). *Management and Analysis of Biological Populations*. Elsevier, Nether-lands.

Guckenheimer, J., & Holmes, P. (1985). *Nonlinear Oscillations, Dynamical Systems, and Bifurcations of Vector Fields*. Springer-Verlag, NY.

Hadeler, K. P., & Gerstmann, I. (1990). *The discrete Rosenzweig model*. Mathematical Biosciences, 98(1), 49–72.

He, Z., & Lai, X. (2011). Bifurcation and chaotic behavior of a discrete-time predator prey systemstar, *Nonlinear Analysis: Real World Applications*, 12, 403–417.

Hastings, A. (1981). Multiple limit cycles in predator-prey models. *Journal of Mathematical Biology*, 11(1), 51–63.

Holling, C. S. (1965). The functional response of predator to prey density and its role in mimicry and population regulation. *Memoirs of the Entomology.* Society *of Canada*, 45, 1–60.

Jiao, J. J., Chen, L. S., Nieto, J. J., & Angela, T. (2008). Permanence and global attractivity of stage-structured predator-prey model with continuous harvesting on predator and impulsive stocking on prey. *Applied* Mathematics *and Mechanics (English Edition),* 29(5) 653–663.

Jiao, J. J., Meng, X. Z., & Chen, L. S. (2008). Global attractivity and permanence of a stage-structured pest management SI model with time delay and diseased pest impulsive transmission. *Chaos Solitons Fractals*, 38(3) 658–668.

Jing, Z., & Yang, J. (2006). Bifurcation and chaos in discrete-time predator-prey system. Chaos, *Solitons and Fractals*, 27(1) 259–277.

Kuang, Y. (1993). *Delay Differential Equations with Applications in Population Dynamics*. Academic Press, New York.

Kooij, R. E., & Zegeling, A. (1997). Qualitative properties of two-dimensional predator-prey systems. *Nonlinear Analysis*, 29(6) 693–715.

Kraft, R. L. (1999). Chaos, Cantor Sets, and Hyperbolicity for the Logistic Maps. *American Mathematical Monthly*, 106(5), 400–408.

Kuznetsov, Yu. A. (2004). *Elements of Applied Bifurcation Theory*. Springer-Verlag, New York.

Kuznetsov Yu. A., & Meijer, H. G. E. (2005). Numerical normal forms for codim 2 bifurcations of maps with at most two critical eigenvalues. *Siam Journal* on *Scientific Computing*, 26(6), 1932–1954.

Kuznetsov Yu. A., & Meijer, H. G. E. (2006). *Remarks on interacting Neimark- Sacker bifurcations, Preprint nr*. 1342, Department of Mathematics, Utrecht University, The Netherlands.

Lauwerier, H. A. (1986). Two-dimensional iterative maps, Chaos, Nonlinear Science. *Theory Application of Manchester University Press, Manchester*, 32, 58–95.

Liu, X., & Xiao, D. (2007). Complex dynamic behaviors of a discrete-time predator-prey system. *Chaos, Solitons and Fractals*, 32(1), 80–94.

Lindstrom, T. (1993). Qualitative analysis of a predator-prey systems with limit cycles. *Journal of Mathematics Biology*, 31(6), 541–561.

Lotka, A. J. (1956). *Elements of Mathematical Biology*, Dover, New York.

Murray, J. D. (1993). *Mathematical Biology*. Berlin, Heidelberg, New York: Springer.

Rosenzweig, M., & MacArthur, R. (1963). Graphical representation and stability conditions of predator-prey interactions. *American Naturalist*, 97(895), 209–23.

Volterra, V. (1962). *Opere Matematiche*. Memoriee Note, Nazionale dei Lincei, Rome, Cremona.

Wang, W. B., Shen, J. H., & Nieto, J. J. (2007). Permanence and periodic solution of predator-prey system with Holling type functional response and impulses. *Discrete* Dynamics in *Nature and Society*, doi: 10. 1155/2007/81756.

Wang, J., Zhou, X., & Huang, L. (2013). Hopf bifurcation and multiple periodic solutions in Lotka-Volterra systems with symmetries, *Nonlinear Analysis: Real World Applications*, 14(3), 1817–1828.

Zeng, G. Z., Wang, F. Y., & Nieto, J. J. (2008). Complexity of a delayed predator-prey model with impulsive harvest and Holling type II functional response, *Advances in Complex System*, 11(1), 77–97.